Submitted: 16 April, 2024 Accepted: 05 July, 2024 Published: 30 July, 2024 DOI:10.22514/jomh.2024.117

ORIGINAL RESEARCH

JOMH Journal of Men's Health

Significance of ultrasonography combined with shear wave elastography in the diagnosis of prostate cancer

Yang Yang[1], Li Zhang[1,*], Chunlai Zhang[1]

[1]Department of Ultrasonic, Lishui People's Hospital, 323000 Lishui, Zhejiang, China

***Correspondence**
zlll039@163.com
(Li Zhang)

Abstract

In order to explore the diagnostic value of ultrasound combined with shear wave elastography (SWE) for prostate cancer (PCa), 120 patients with suspected prostate cancer were selected for SWE, contrast-enhanced ultrasound (CEUS), SWE and CEUS combined examination. The results showed that among the 120 patients, 57 cases were diagnosed as prostate cancer and 63 cases as benign prostatic lesions by biopsy. Among 58 cases of PCa diagnosed by SWE, 46 cases were confirmed by pathology, with a sensitivity of 80.70% and a specificity of 77.20%. Among 54 cases of PCa diagnosed by CEUS, 41 cases were confirmed by pathology, with a sensitivity of 80.70% and a specificity of 77.20%. 61 patients with PCa were diagnosed by we and CEUS, and 51 patients were diagnosed by pathology. The sensitivity, specificity and accuracy were 89.47%, 84.70% and 85.38%, respectively. Receiver operating characteristic (ROC) curve results showed that the area under the curve (AUC) of swe and CEUS was 0.944, showing the highest diagnostic efficacy. It can be seen that the combined use of SWE and CEUS provides a more superior diagnostic effect for PCa.

Keywords

Prostate cancer; Shear wave elastography; Ultrasonography; Diagnostic value

1. Introduction

Prostate cancer (PCa) is one of the most common malignant tumors in the male reproductive system, ranking as the second most prevalent malignant tumor in men globally [1]. By 2022, there were 1.91 million new cancer cases and 610,000 cancer deaths in the United States [2]. Prostate, lung and colorectal cancers account for 48% of new cases, with PCa representing 27% of new cases in men. Among them, PCa is one of the most common tumors in men, accounting for the highest number of new cases and deaths [3]. Its incidence has been found to be positively correlated with the human development index and economic level [4]. Global cancer data indicate a significant increase in the incidence of male PCa in recent years, with China, an East Asian country, continuing to have a large number of undiagnosed PCa patients [5].

In China, the number of tumor patients has been increasing annually, with PCa accounting for 60% of new cases and 89% of fatalities, making it one of the fastest-growing tumors [6]. Although PCa is less common in China than in Europe or the US, the disease has become more prevalent and poses a serious threat to men's health due to the country's aging population, increasing urbanization, westernization of dietary habits, and gradual promotion of serum prostate-specific antigen (PSA) screening over the past decade [7, 8]. The clinical diagnosis of PCa is primarily based on patients' clinical manifestations, levels of relevant indicators, rectal examination and nuclear magnetic resonance imaging.

In recent years, ultrasonography technology has developed rapidly, and some scholars have used transrectal ultrasonography for diagnosing PCa. However, previous studies have shown that this method has varying degrees of error [9]. To improve the clinical diagnosis rate, it is necessary to combine effective imaging techniques for screening patients with prostate disease [10]. Previous reports on PCa patients have mostly used contrast-enhanced ultrasound (CEUS) alone, without combining it with other imaging techniques. The imaging quality of CEUS alone is not high, significantly impacting diagnostic results [11, 12]. In this regard, shear-wave elastography (SWE) is a commonly used imaging technique that can quantitatively detect Young's modulus value of tissues, reflecting tissue hardness [13].

This study aimed to analyze the diagnostic efficacy of three protocols for PCa using CEUS alone, SWE and their combination.

2. Information and methods

2.1 General information

The clinical data from 120 patients with suspected PCa who underwent prostate ultrasound examination at our hospital between January 2021 and July 2023 were retrospectively analyzed.

The inclusion criteria comprised cases with no previous

This is an open access article under the CC BY 4.0 license (https://creativecommons.org/licenses/by/4.0/).
 ©2024 The Author(s). Published by MRE Press.

prostate surgery, a prostate volume of less than 80 mL as determined by B ultrasound, and no signs of extracapsular infiltration. Those with contraindications to prostate biopsy, prior treatment for PCa, acute phase urinary infection, urinary tract infections, severe coagulation abnormalities, other malignancies, psychiatric disorders, or cognitive impairment were excluded from the study analysis.

All patients underwent SWE and CEUS before prostate biopsy.

2.2 Methods

2.2.1 Clinical data collection

The baseline patient information, including age, body mass index, and smoking history, was retrieved. Enzyme-linked immunosorbent assay was performed to assess their serum PSA levels at the time of admission. A total serum PSA $\leq$4 ng/mL was considered normal, with elevated total serum PSA suggesting the possibility of PCa [14].

2.2.2 Instrumentation

SWE and CEUS were performed using AixPlorer ultrasonic diagnostic instruments (French Supersonic Imagine Company, SE12-3 intracavitary probe, frequency of 3–12 MHz, low mechanical index, AIX Provence, France). Puncture biopsy utilized the LOGIQ-E8 ultrasonic diagnostic instrument (GE Healthcare investment (China) Co., Ltd., frequency of 5–9 MHz intracavitary probe, Pudong New Area, Shanghai, China), equipped with a special intracavitary probe and puncture frame, using disposable BARD equipment. The puncture rack employed a fully automated biopsy gun with disposable BARD 18 G $\times$ 25 cm size.

2.2.3 Inspection methods

2.2.3.1 Pre-examination preparation

The electrocardiogram (ECG), blood routine, coagulation profile, infection status and liver and kidney functions were assessed and met the puncture criteria. There were no contraindications. A clean enema was administered prior to the procedure, and the bladder was emptied.

2.2.3.2 SWE examination method

The patient was positioned on his left side, breathing deeply, bending his knee to his chest, and clasping it with both hands. Initially, rectal two-dimensional ultrasound was used to examine the outline and echo of the prostate. If nodules were detected, their two-dimensional state was assessed, and flow Doppler was used to evaluate blood flow. Once the image was stabilized, the SWE mode was activated. The patient was instructed to hold his breath, and the image was frozen. The Q-BOX TM function measurement tool was used to determine the modulus of elasticity (Emax) value of the region of interest. Each lesion was measured three times to collect three sets of data. The average value of these three sets was then calculated and stored.

2.2.3.3 Methods of CEUS examination

The Sonovue contrast agent (20A048, BRACCORegistration agency of overseas produced drugs, bleco Pharmaceutical Technology (Shanghai) Co., Ltd., Jing'an District, Shanghai, China) was utilized. The patient's antecubital fossa was routinely sterilized, and an intravenous access was established. The patient was positioned in a similar manner as for the SWE examination and instructed to breathe calmly. Initially, transrectal two-dimensional ultrasonography was performed to observe the size, morphology and internal echogenicity of the prostate gland. If nodules were detected, their two-dimensional characteristics and color blood flow were evaluated. If no suspicious nodules were found, the largest cross-section was selected and held still for examination. The CEUS mode was then activated, and 2.5 mL of Sonovue contrast agent was injected through the intravenous channel, followed by 5 mL of saline. The contrast in the suspicious area of the prostate gland was observed, recorded and stored.

2.2.3.4 Puncture biopsy method

The patient was positioned in the left lateral position, with the knee bent and leg held to fully expose the anus. The anterior end of the ultrasound probe, coated with a coupling agent, was routinely disinfected with 0.5% iodophor. A transrectal puncture frame was installed after wrapping the probe with a contraceptive sleeve. The probe was slowly inserted, and a "12+X" puncture method was used. An additional 2–3 punctures were conducted in atypical locations indicated by elasticity and contrast. If no suspicious areas were identified, no extra punctures were performed. Tissue strips from the systematic puncture and those showing suspected anomalies on SWE and CEUS were placed in individually labeled containers with 10% formaldehyde and promptly sent for evaluation.

All procedures were performed by two senior ultrasonographers to minimize human error.

2.3 Diagnostic criteria

SWE: The receiver operating characteristic (ROC) curve was used to determine the optimal cutoff value of each SWE parameter for diagnosing benign and malignant lesions. The parameter with the best efficacy was selected as the cutoff value. Values below the cutoff were defined as benign and those above as malignant [15].

CEUS: PCa was diagnosed based on the following criteria: (1) rapid contrast uptake and washout with high enhancement; (2) inhomogeneous enhancement with poorly defined borders; (3) asymmetric vascular structures. These features suggest a malignant lesion [16].

Pathologic Findings: The Gleason score from Epstein's criteria was used to classify PCa into significant PCa (Gleason score $>$6) and non-significant PCa (Gleason score $\leq$6) [17].

2.4 Statistical analysis

The SPSS v20.0 software (SPSS Inc., Chicago, IL, USA) was used for statistical analysis. Measurement data are described using mean $\pm$ standard deviation ($\bar{x} \pm s$), count data are described using rates, and statistical comparison was performed using the χ^2 test. ROC curves were used to determine the optimal cutoff value of Emax for the diagnostic value of PCa using SWE. The sensitivity, specificity, and area under the curve (AUC) of CEUS, SWE and their combined application

TABLE 1. General information of 120 patients.

Group	Age (yr)	BMI (kg/m^2)	PSA (ng/mL)	Smoking history (n/%)
PCa (n = 57)	60.63 ± 5.18	23.61 ± 3.60	48.80 ± 4.96	42 (73.68)
Benign prostate lesions (n = 63)	61.59 ± 6.66	23.23 ± 3.06	8.90 ± 1.03	41 (65.08)
t/χ^2	0.880	0.623	62.438	1.039
p	0.381	0.534	<0.001	0.308

BMI: Body Mass Index; PSA: prostate-specific antigen; PCa: Prostate cancer.

for diagnosing PCa were calculated, and significance level of the test was set at $\alpha = 0.05$.

3. Results

3.1 Pathologic results

Data analysis showed there were 63 benign prostate cases (52.50%) and 57 PCa patients (47.50%) among the 120 patients, with 19 patients having non-significant PCa and 38 having significant PCa. Pathological puncture results of the 57 patients with malignant tumors indicated that 35 patients (61.40%) had nodules in the peripheral zone, 13 patients (22.80%) had nodules at the junction of the inner and outer limits, and the remaining had nodules at the inner limits (15.79%). The clinical data of the 120 patients are detailed in Table 1.

3.2 Diagnostic efficacy of SWE compared with pathologic findings

SWE identified 58 patients with suspected PCa, 46 of whom were confirmed by pathologic diagnosis, resulting in 12 cases of misdiagnosis. When Emax was 47.158 kPa, Youden's index was the highest, with a sensitivity of 80.70%, specificity of 77.20%, and accuracy (Youden's index) of 75.60%. The results are detailed in Table 2.

TABLE 2. Diagnostic efficacy of SWE compared to pathological findings.

SWE	Biopsy results		Jordon's index (%)
	Malignant (n = 57)	Benign (n = 63)	
Malignant (n = 58)	46	12	75.60
Benign (n = 62)	11	51	

SWE: shear wave elastography.

3.3 Diagnostic efficacy of CEUS compared with pathologic findings

CEUS identified 54 patients with suspected PCa, 41 of whom were confirmed by pathologic diagnosis, resulting in 12 cases of misdiagnosis (Table 3). The diagnostic sensitivity was 71.93%, specificity was 68.40%, and accuracy was 70.20%. The results showed that although the diagnostic efficacy of CEUS was lower compared to SWE, the difference between groups was not significant ($\chi^2 = 1.728$, $p = 0.189$).

TABLE 3. Diagnostic efficacy of CEUS compared with pathological findings.

CEUS	Biopsy results		Jordon's index (%)
	Malignant (n = 57)	Benign (n = 63)	
Malignant (n = 54)	41	13	70.20
Benign (n = 66)	16	50	

CEUS: contrast-enhanced ultrasound.

3.4 Diagnostic efficacy of SWE when combined with CEUS compared with pathologic results

SWE combined with CEUS identified 61 patients with suspected PCa, 51 of whom were confirmed by pathologic diagnosis, resulting in 10 cases of misdiagnosis (Table 4), resulting in a sensitivity of 89.47%, specificity of 84.70%, and an accuracy of 85.38%.

TABLE 4. Diagnostic efficacy of SWE combined with CEUS compared to pathologic results.

SWE combined with CEUS	Biopsy results		Jordon's index (%)
	Malignant (n = 57)	Benign (n = 63)	
Malignant (n = 61)	51	10	85.38
Benign (n = 59)	6	53	

SWE: shear wave elastography; CEUS: contrast-enhanced ultrasound.

3.5 Comparison of diagnostic efficacy of SWE combined with CEUS for PCa

The AUC for all three methods was greater than 0.5, as shown by the ROC curves, indicating high diagnostic efficacy. However, the combination of SWE and CEUS exhibited even higher sensitivity and specificity compared to the individual methods, demonstrating the highest diagnostic efficacy for PCa (Table 5 and Fig. 1).

4. Discussion

Although the incidence of PCa in China is lower than that in Western countries, its incidence has been increasing in

TABLE 5. Comparison of the diagnostic efficacy of SWE and CEUS separately and in combination for PCa diagnosis.

Method	Sensitivity	Specificity	AUC (95% CI)
SWE	80.70	77.20	0.929 (0.877–0.981)
CEUS	71.93	68.40	0.832 (0.745–0.917)
SWE combined with CEUS	89.47	84.70	0.944 (0.899–0.988)

AUC: area under the curve; CI: confidence interval; SWE: shear wave elastography; CEUS: contrast-enhanced ultrasound.

China in recent years [18]. Thus, improving the accuracy of early diagnosis, along with effective surgical treatment, can significantly improve the prognosis of PCa patients [19]. According to statistics, the 5-year survival rate of some PCa patients after radical treatment can be as high as 99% [20]. Although the risk factors for PCa are not yet fully understood, epidemiological studies indicate that men over 40, particularly Caucasians and Blacks, due to genetic predisposition, are more susceptible, and additional independent risk factors include smoking, obesity and diabetes [21, 22]. Therefore, improving the diagnostic accuracy of PCa and providing timely treatment to reduce mortality is crucial in clinical research. Currently, systematic puncture biopsy is the most commonly used method to diagnose PCa. However, it has low sensitivity and specificity, is traumatic for patients, and can cause complications [23].

CEUS utilizes the nonlinear effect and backscattering of contrast agent microbubbles in the blood to produce contrast-enhanced images, thereby revealing the microcirculatory perfusion of tissues [24]. Both domestic and international research in prostate angiography have shown that tumor growth significantly increases the microvascular density within PCa. However, these vessels are typically small, thin-walled, have low blood flow velocity, and may contain arterial fistulae, making them undetectable by conventional color Doppler ultrasound [25]. Studies have indicated that CEUS can accurately locate suspicious malignant nodes in the prostate and reflect the Gleason score and extent of the tumor [26]. SWE, a novel ultrasound imaging technology, uses color-coded technology

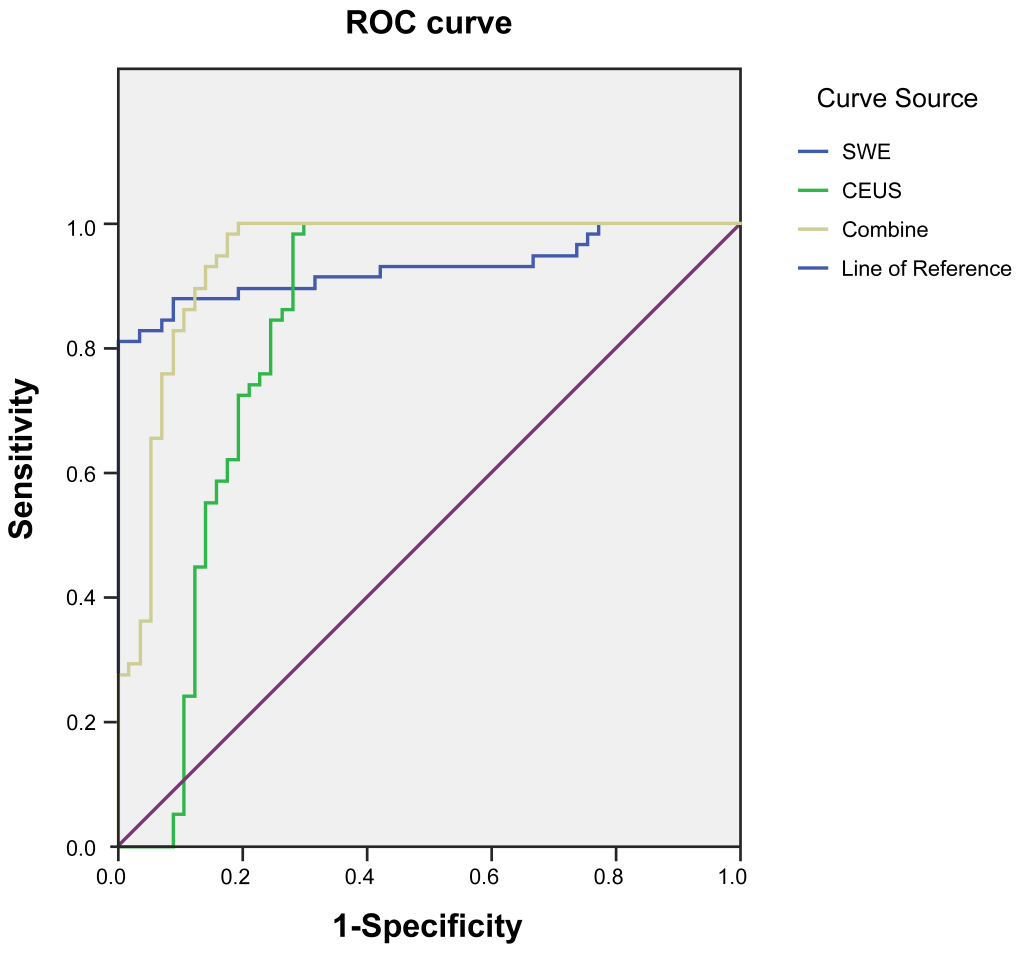

FIGURE 1. ROC curves of SWE and CEUS separately and in combination for PCa diagnosis. ROC: receiver operating characteristic; SWE: shear wave elastography; CEUS: contrast-enhanced ultrasound.

to quantitatively assess tissue hardness based on internal elasticity, with different colors representing varying degrees of stiffness [27]. There is a strong correlation between the *E*-value of SWE and the Gleason score of pathology, suggesting that a lower degree of differentiation (higher malignancy) in PCa corresponds to a higher *E*-value. This indicates that SWE has a higher diagnostic value for detecting highly malignant PCas [28]. Additionally, studies have demonstrated that SWE has a higher positive detection rate for PCa compared to conventional transrectal ultrasound [29].

This study uses the pathological results of a prostate biopsy as the gold standard to assess the efficacy of CEUS, SWE, and their combined application in the diagnosis of PCa. The findings indicate that the sensitivity, specificity and accuracy of PCa diagnosis with SWE or CEUS are comparable, with SWE slightly outperforming CEUS, though the difference is not significant. However, the combined use of SWE and CEUS significantly improves diagnostic performance, with a sensitivity of 89.47%, specificity of 84.70%, and accuracy of 85.38%. The ROC curve analysis showed that the AUC for the combined use of SWE and CEUS was 0.944, significantly higher than the AUC for SWE (0.929) and CEUS (0.832). This indicates that the combined application of SWE and CEUS has the highest diagnostic efficacy among the three methods, offering new hope for the diagnosis of PCa.

This study had several limitations that should be considered, such as a small sample size and incomplete data, which might have affected the interpretation of the findings to a certain extent. Furthermore, the investigation considered fewer factors and focused on elderly patients. Therefore, increasing the sample size and further exploration of the research topic are essential for future studies.

5. Conclusions

In summary, CEUS is an effective imaging technology for diagnosing benign and malignant prostate lesions, while SWE uses the absolute elastic value (Young's modulus) to assess tissue stiffness. Both technologies have significant clinical value in treating prostate diseases. However, the combined application of CEUS and SWE in diagnosing PCa is significantly more effective than using each technology individually.

AVAILABILITY OF DATA AND MATERIALS

The authors declare that all data supporting the findings of this study are available within the paper and any raw data can be obtained from the corresponding author upon request.

AUTHOR CONTRIBUTIONS

YY—designed the study and carried it out; YY and LZ—supervised the data collection, analyzed the data, and interpreted the data; YY, LZ and CLZ—prepared the manuscript for publication and reviewed the draft of the manuscript. All authors have read and approved the manuscript.

ETHICS APPROVAL AND CONSENT TO PARTICIPATE

Ethical approval was obtained from the Ethics Committee of Lishui People's Hospital (Approval no. LLW-FO-403). This retrospective study was approved by an ethics review board, and the requirement to obtain informed written consent was waived.

ACKNOWLEDGMENT

Not applicable.

FUNDING

This research received no external funding.

CONFLICT OF INTEREST

The authors declare no conflict of interest.

REFERENCES

[1] Liu L, Sun FZ, Zhang PY, Xiao Y, Yue X, Wang DM, *et al.* Primary high-grade urothelial carcinoma of prostate with prostatic hyperplasia: a rare case report and review of the literature. Aging Male. 2023; 26: 2252102.

[2] Surintrspanont J, Zhou M. Prostate pathology: what is new in the 2022 WHO classification of urinary and male genital tumors? Pathologica. 2023; 115: 41–56.

[3] Low JY, Ko M, Hanaratty B, Patel RA, Bhamidipati A, Heaphy CM, *et al.* Genomic characterization of prostatic basal cell carcinoma. American Journal of Pathology. 2023; 193: 4–10.

[4] Netto GJ, Amin MB, Berney DM, Compérat EM, Gill AJ, Hartmann A, *et al.* The 2022 world health organization classification of tumors of the urinary system and male genital organs-part B: prostate and urinary tract tumors. European Urology. 2022; 82: 469–482.

[5] Pokhrel A, Heravi O, Enayati L, Nelson R, Mooppan U, Wu RC, *et al.* Association between prostate carcinoma and multiple myeloma. Discovery Medicine. 2023; 35: 664–672.

[6] Zhu S, Zhao JG, Nie L, Yin WL, Zhang YW, Zhao FN, *et al.* Homologous recombination deficiency (HRD) score in aggressive prostatic adenocarcinoma with or without intraductal carcinoma of the prostate (IDC-P). BMC Medicine. 2022; 20: 237.

[7] Han M, Li FI, Zhang YH, Dai PF, He J, Li YG, *et al.* FOXA2 drives lineage plasticity and KIT pathway activation in neuroendocrine prostate cancer. Cancer Cell. 2022; 40: 1306–1323.e8.

[8] Chen CC, Tran W, Song K, Sugimoto T, Obusan MB, Wang L, *et al.* Temporal evolution reveals bifurcated lineages in aggressive neuroendocrine small cell prostate cancer trans-differentiation. Cancer Cell. 2023; 41: 2066–2082.e9.

[9] Lin XQ, Shi QY, Yang XJ. Cytomorphology, immunoprofile, and clinicopathologic correlation of metastatic prostatic carcinoma. Human Pathology. 2022; 130: 36–46.

[10] Tariq A, Reed AEM, Morton A, Porten S, Vela I, Williams ED, *et al.* Urothelial carcinoma and prostate-specific membrane antigen: cellular, imaging, and prognostic implications. European Urology Focus. 2022; 8: 1256–1269.

[11] Jia L, Bin H, Bing H, Jin H. CEUS examination of the outcome of radiofrequency ablation of canine prostate lesions. Minimally Invasive Therapy & Allied Technologies. 2021; 30: 334–340.

[12] Kunikowska J, Cieslak B, Gierej B, Patkowski W, Kraj L, Kotulski M, *et al.* [^{68} Ga]Ga-prostate-specific membrane antigen PET/CT: a novel method for imaging patients with hepatocellular carcinoma. European Journal of Nuclear Medicine and Molecular Imaging. 2021; 48: 883–892.

[13] Licen U, Kozinc Z. Using shear-wave elastography to assess exercise-induced muscle damage: a review. Sensors. 2022; 22: 7574.
[14] Epstein JI, Amin MB, Fine SW, Algaba F, Aron M, Baydar DE, *et al.* The 2019 genitourinary pathology society (GUPS) white paper on contemporary grading of prostate cancer. Archives of Pathology & Laboratory Medicine. 2021; 145: 461–493.
[15] Tyloch DJ, Tyloch JF, Adamowicz J, Neska-Dlugosz I, Grzanka D, Van Breda S, *et al.* Comparison of strain and shear wave elastography in prostate cancer detection. Ultrasound in Medicine and Biology. 2023; 49: 889–900.
[16] Gupta R, Mahajan M, Sharma P. Correlation between prostate imaging reporting and data system version 2, prostate-specific antigen levels, and local staging in biopsy-proven carcinoma prostate: a retrospective study. International Journal of Applied and Basic Medical Research. 2021; 11: 32–35.
[17] Pham THN, Schulze-Hagen MF, Rahnama'i MS. Targeted multi-parametric magnetic resonance imaging/transrectal ultrasound-guided (mpMRI/TRUS) fusion prostate biopsy versus systematic random prostate biopsy: a comparative real-life study. Cancer Reports. 2024; 7: e1962.
[18] Zong Y, Montironi R, Massari F, Jiang Z, Lopez-Beltran A, Wheeler TM, *et al.* Intraductal carcinoma of the prostate: pathogenesis and molecular perspectives. European Urology Focus. 2021; 7: 955–963.
[19] de Kouchkovsky I, Chan EMY, Schloss C, Poehlein C, Aggarwal R. Diagnosis and management of neuroendocrine prostate cancer. Prostate. 2024; 84: 426–440.
[20] Kalampokis N, Grivas N, Karavitakis M, Leotsakos I, Katafigiotis I, Moschovas MC, *et al.* Nondetectable prostate carcinoma (pT0) after radical prostatectomy: a narrative review. Current Oncology. 2022; 29: 1309–1315.
[21] Gandaglia G, Leni R, Bray F, Fleshner N, Freedland SJ, Kibel A, *et al.* Epidemiology and prevention of prostate cancer. European Urology Oncology. 2021; 4: 877–892.
[22] Bergengren O, Pekala KR, Matsoukas K, Fainberg J, Mungovan SF, Bratt O, *et al.* 2022 update on prostate cancer epidemiology and risk factors—a systematic review. European Urology. 2023; 84: 191–206.
[23] Dorfinger J, Ponholzer A, Stolzlechner M, Lenart S, Baltzer P, Toepker M. MRI/ultrasound fusion biopsy of the prostate compared to systematic prostate biopsy—effectiveness and accuracy of a combined approach in daily clinical practice. European Journal of Radiology. 2022; 154: 110432.
[24] Dias AB, O'Brien C, Correas JM, Ghai S. Multiparametric ultrasound and micro-ultrasound in prostate cancer: a comprehensive review. British Journal of Radiology. 2022; 95: 20210633.
[25] Gurwin A, Kowalczyk K, Knecht-Gurwin K, Stelmach P, Nowak L, Krajewski W, *et al.* Alternatives for MRI in prostate cancer diagnostics—review of current ultrasound-based techniques. Cancers. 2022; 14: 1859.
[26] Keskin ET, Kaplanoglu V, Senocak C, Basar H, Bozkurt OF. Transrectal shear wave elastography for detection of prostate cancer. Urologia Journal. 2023; 90: 230–235.
[27] Secasan CC, Onchis D, Bardan R, Cumpanas A, Novacescu D, Botoca C, *et al.* Artificial intelligence system for predicting prostate cancer lesions from shear wave elastography measurements. Current Oncology. 2022; 29: 4212–4223.
[28] Morris DC, Chan DY, Palmeri ML, Polascik TJ, Foo WC, Nightingale KR. Prostate cancer detection using 3-D shear wave elasticity imaging. Ultrasound in Medicine and Biology. 2021; 47: 1670–1680.
[29] Anbarasan T, Wei C, Bamber JC, Barr RG, Nabi G. Characterisation of prostate lesions using transrectal shear wave elastography (SWE) ultrasound imaging: a systematic review. Cancers. 2021; 13: 122.

How to cite this article: Yang Yang, Li Zhang, Chunlai Zhang. Significance of ultrasonography combined with shear wave elastography in the diagnosis of prostate cancer. Journal of Men's Health. 2024; 20(7): 132-137. doi: 10.22514/jomh.2024.117.